

DECOUPLING CONTROL OF PULLOUT MANEUVER FOR MARS AIRPLANE

YANBIN LIU^{1,*}, KEMING YAO² AND YUPING LU¹

¹College of Astronautics

Nanjing University of Aeronautics and Astronautics
No. 29, Yudao St., Nanjing 210016, P. R. China

*Corresponding author: nuaa.liuyanbin@139.com

²College of Electronic and Information Engineering

Jiangsu Teachers University of Technology
No. 1801, Zhongwu St., Changzhou 213001, P. R. China
nuaa_yaokeming@163.com

Received December 2011; revised September 2012

ABSTRACT. *Mars airplane, which is considered as an important research area of the deep-space exploration because of the wide observation range, flexible maneuverability and high efficiency, has recently been designed and developed to get extended knowledge of the Martian surface. In this paper, the decoupling and switching control problems of pullout maneuver are investigated for Mars airplane. First, the flight characteristics are described by the trim analysis. Then, the decoupling flight control laws of the different flight phases based on the switched system theory are proposed to implement the coordinated and integrated control process. Finally, the effectiveness of the decoupling flight control methods is confirmed by using the numerical simulation, and the results show the flight stability of the pullout maneuver can be guaranteed.*

Keywords: Mars airplane, Deep-space exploration, Switching control, Flight control, Dynamic characteristics

1. Introduction. Human beings have explored Mars for many years because it is one of the closest planets to the earth in our own solar system. A large number of Mars probes have been designed and developed to help humans understand the unknown field. By using them, there are some fruitful results acquired to the scientific research. Specifically, NASA launching the Mars exploration plans, called the Aerial Regional-scale Environmental Survey (ARES), will inspire a new upsurge on Martian scientific study. The goal of ARES is to obtain Mars resource information that cannot be captured from either ground vehicles or orbiters [1]. In the past few decades, the orbital detectors have achieved many valuable results. However, the orbital platforms and robots are subjected to the mobility and flexibility of the detecting motion [2]. Whereas an airplane offers an additional advantage over other platforms in that it can be maneuvered to specific locations of interest [3]. In addition, an airplane with potential application to Mars can also bridge the scale and resolution measurement gaps between orbiters and landers [4]. More importantly, there are some scientific goals to realize, for example, conducting a high resolution magnetic survey of the Mars Southern Highlands, analyzing the atmospheric gases and studying the mineralogy of the oldest crust in the solar system [4]. However, Mars airplane design, which involves a number of challenges that are not encountered in the design of the earth airplane, presents unique challenges caused by the complicated Martian atmosphere and low Reynolds number. At the same time, the transonic aerodynamic effects are encountered at a lower flight speed because the speed of sound on Mars is lower than

that on Earth, whereas the lower atmospheric density leads to the higher cruise speed, so special care must be taken in the aerodynamic design to avoid dramatic losses in the lift and dramatic increases in drag associated with the low Reynolds number, high Mach number flight conditions [5]. In general, the Mars exploration has become the important research direction of the deep-space exploration, but it is very challenging to realize the expected goals [2].

The crucial events of Mars airplane represent new research directions, including the extraction of the airplane from the aeroshell, the deployment to flight configuration, and the pullout to level flight in a thin atmosphere [6]. Specifically, the Monte-Carlo dispersion resulting from the multi-body dynamics simulation, which consists of nine bodies and encompasses the critical events following main parachute deployment and preceding autonomous flight, are obtained to determine the altitude range at which the aircraft can be expected to begin level flight operations [7]. Then, the flight trajectory is developed to maximize the surface-relative altitude of the airplane at the end of a pullout maneuver, and the analysis shows that if more capability is needed during the pullout maneuver, airfoils with the highest lift coefficients must be selected [8]. Moreover, based on a mathematical model of the ARES aircraft built, a longitudinal reference-tracking flight control system is designed to achieve or surpass the given control performance requirements [9]. Also, the control system of Mars airplane is presented with a blend of H^∞ and proportional-integral controllers in order to improve the aircraft robustness [10]. After that, the control studies are performed in the frame the design, development, test, and evaluation of the GNC of a Mars Sample Return and Mars vehicles [11].

The fundamental issues for switched linear systems focus on controllability, observability, feedback stabilization, optimization and feasible switching [12]. Especially, average dwell time method [13] is used to achieve the exponential stability for switched systems. Based on this method, the stability analysis problems are investigated for the switched positive linear systems [14], an impulsive switched system with time delay [15], switched neural networks with time-varying delay [16], switched LPV system [17] and discrete-time switched systems with average dwell time [18]. Furthermore, there are some expand applications associated with the stability analysis of switched systems, such as asynchronous H-infinity control [18], robust fault detection [19] and asynchronous H-infinity filtering [20]. The crucial events of Mars airplane are related to the switching process, thus the stability and control problems for switched systems need to be addressed for the pullout maneuver of Mars airplane. In fact, the key to a successful pullout is the lift of the airplane which determines the effectiveness of the switching control action. In addition, the decoupling and switching control system, which is employed for Mars airplane to decrease the speed and orient itself, will make the aircraft possible to traverse well into the transonic flight regime and meet the needs of the pullout to level flight in a thin atmosphere.

In this paper, the switching control problems of pullout maneuver for Mars airplane are researched. The first question involves the trajectory plan of pullout maneuver based on Mars environment to provide the scheduled control missions. The second problem relates to the control law design using the switched system methods such that the vehicle model established realizes the smooth transition with regard to the orientation maneuver, pullout maneuver and level flight. The third aspect deals with the stability analysis of the switching control, and then the simulation examples demonstrate the effectiveness and feasibility of the proposed methods.

2. Fight Environment Description and Modeling on Mars. Mars atmosphere contains largely of carbon dioxide with small amounts of argon and nitrogen such that the atmospheric density on the surface is approximately equal to the air density of 30km

altitude on Earth. Thus, the lift of Mars aircraft is obviously inadequate, but fortunately, the mass of Mars is only 11% of the mass of Earth such that the gravity on Mars is only two-fifths of the gravity on Earth [21]. Correspondingly, the trimmed horizontal flight can be achieved when the vehicle speed reaches a certain range. Nevertheless, the conventional turbine engine cannot work due to lack of oxygen in the Martian atmosphere, so the rocket propulsion system applied will add the extra loads that have unfavorable effects on the long cruise mission. Luckily, the small thrust is enough to compensate the drag linked to the low atmospheric density. So the temperature, speed of sound and pressure of Mars atmosphere as a function of altitude can be provided by [9]

$$\begin{cases} T(h) = T_0 + T_s h \\ a = \sqrt{\gamma \cdot R_m \cdot T} \\ P(h) = P_0 \cdot e^{P_s \cdot h} \end{cases} \quad (1)$$

where $T_0 = 249.75\text{K}$, $T_s = -2.22 \times 10^{-3}\text{K/m}$, $R_m = 191.8(\text{N} \cdot \text{m})/(\text{kg} \cdot \text{K})$, $P_0 = 699\text{Pa}$, $P_s = -9 \times 10^{-5}\text{m}^{-1}$. The contrast curves between on Mars and on earth are shown in Figure 1.

Furthermore, the relationship of the density and gravity constant with regard to the altitude is given by [10]

$$\begin{cases} \rho = \frac{P}{R_m \cdot T} \\ g_{Mars} = G \cdot \frac{M_{Mars}}{(R_{Mars} + h)^2} \end{cases} \quad (2)$$

where $G = 6.67 \times 10^{-11}(\text{N} \cdot \text{m}^2)/\text{kg}^2$, $M_{Mars} = 6.42 \times 10^{23}\text{kg}$, $R_{Mars} = 3397\text{km}$. The contrast curves of the density and the gravity constant are plotted in Figure 2.

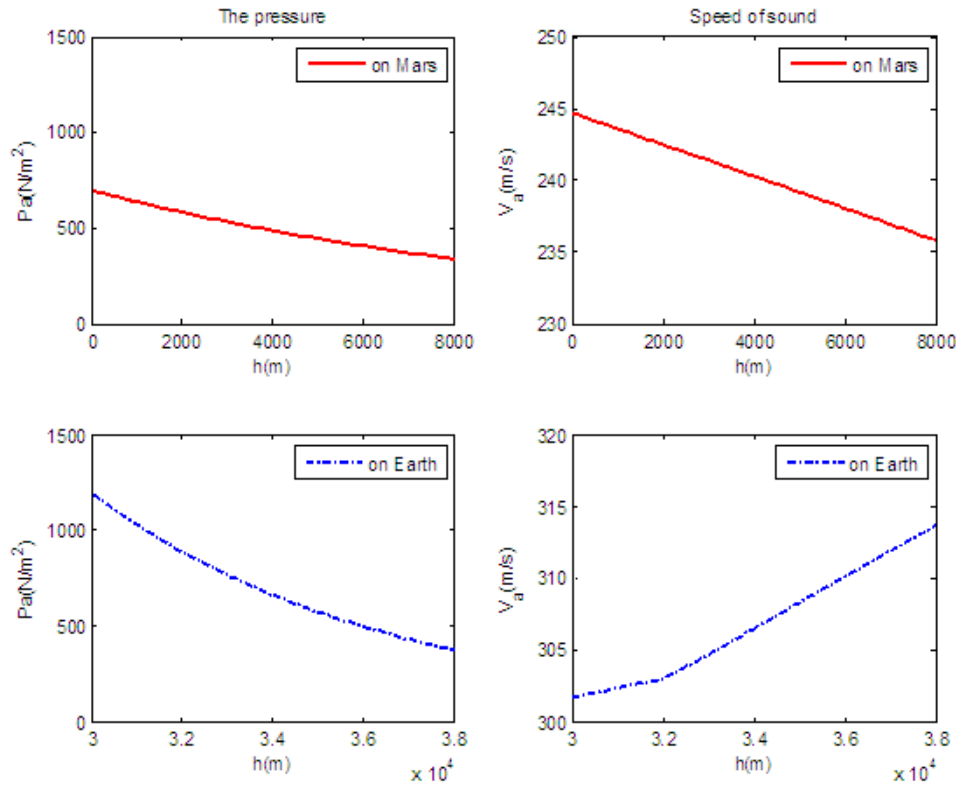


FIGURE 1. Contrast curves of the pressure and speed of sound

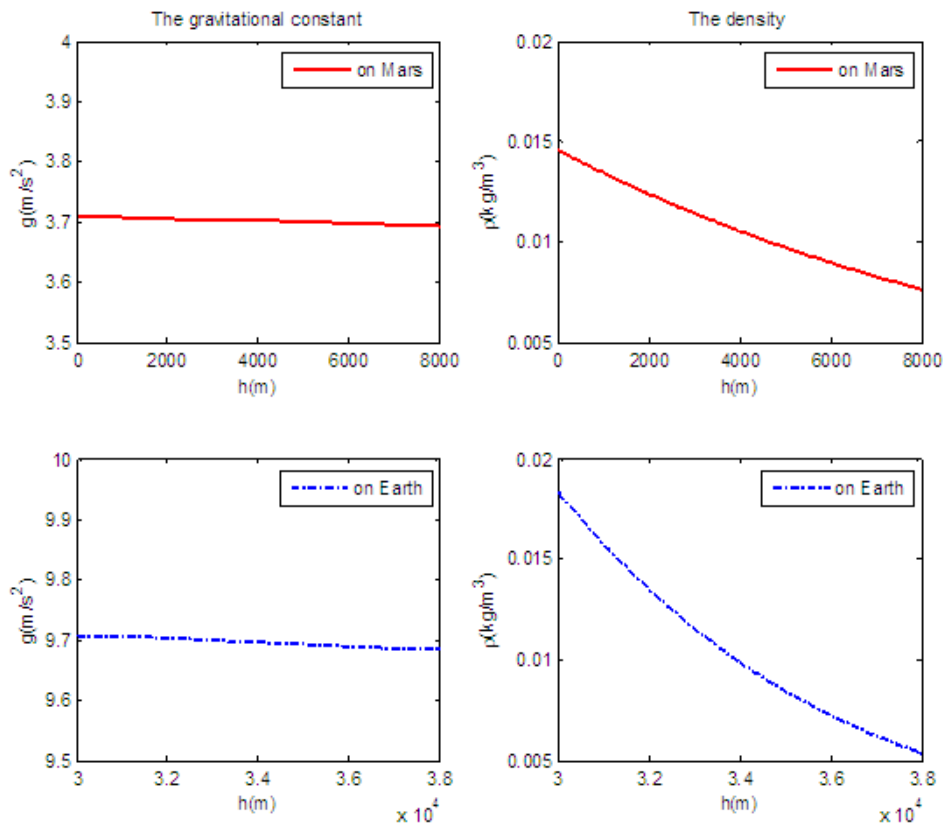


FIGURE 2. Contrast curves of the gravitational constant and density

From the above figures, the atmospheric pressure at the surface of Mars and that at 33.5km above the Earth's sea level are almost the same. In addition, the air density above the surface of Mars is similar to that at 30kms above the Earth. Thus, in future flying an autonomous, powered demonstrator in the Earth's atmosphere at an altitude of approximately 30kms can simulate the flight process and test the analogue flight performance effectively for Mars airplane. In fact, the speed of sound on Mars is lower than that on Earth such that transonic aerodynamic effects will appear at a lower speed. Furthermore, Mars airplane weight is only 38% of what it would be on Earth due to the lower gravitational constant on Mars, so the gravitational pullout is nearly one-third that of Earth. As a result, it is a challenging task to solve the control problems of the pullout maneuver with regard to the unusual flight conditions and discontinuous motion states.

3. Mission Description and Route Plan for Mars Airplane. A typical mission of Mars airplane is considered as the sequences that begin with the spacecraft releasing the entry vehicle into the atmosphere. Then the entry vehicle deploys its parachute and begins to decelerate. Meanwhile, the heatshield is released after the entry vehicle has slowed sufficiently [22]. Shortly thereafter, the folded aircraft released from the aeroshell unfolds the tails and wing, and begins its flight. After that, Mars airplane is to arrest its descent and to pull into horizontal flight. Once the pullout maneuver is completed, the airplane will begin its preplanned aerial survey [23]. In this paper, much attention will be concentrated on the pullout maneuver of Mars airplane which needs to rely on the control action to stabilize the flight course. As a result, the main work is to address the

switching control problems associated with the orientation, pullout maneuver and level flight for Mars airplane.

Theoretically, the pullout maneuver is the transient process between the oriented glide and the level flight. Thus planning the reasonable trajectory of pullout maneuver is necessary to ensure the smooth handoff of the different flight states and to provide the command signals for the control action. In this study, the descent rate command (\dot{H}_c) with regard to the altitude command (H_c) is proposed as follows:

$$\dot{H}_c = \begin{cases} \dot{H}_0 & H_c > H_0 \\ \frac{\dot{H}_0(H_c - H_m)}{(H_0 - H_m)} & (H_c \leq H_0) \& (|\dot{H}_c| > \dot{H}_\varepsilon) \\ 0 & |\dot{H}_c| \leq \dot{H}_\varepsilon \end{cases} \quad (3)$$

$$\dot{H}_\varepsilon = \frac{\dot{H}_0(H_p - H_m)}{(H_0 - H_m)} \quad (4)$$

where H_0 and \dot{H}_0 are the initial altitude and descent rate at the pullout stage, respectively, and H_p denotes the given level flight height. In addition, H_m represents the ideal pullout height as $\dot{H}_c = 0$, so the altitude command is obtained by

$$H_c = \begin{cases} H_d - \dot{H}_0 t & H_c > H_0 \\ H_m - (H_m - H_0)e^{\frac{\dot{H}_0}{(H_0 - H_m)}(t - \frac{H_d - H_c}{\dot{H}_0})} & (H_c \leq H_0) \& (|\dot{H}_c| > \dot{H}_\varepsilon) \\ H_p & |\dot{H}_c| \leq \dot{H}_\varepsilon \end{cases} \quad (5)$$

From Equation (5), the planned trajectory includes three parts: the oriented downslide route, pullout route and level flight route. During the pullout maneuver, \dot{H}_c will decrease gradually, when it reaches the threshold value (\dot{H}_ε), \dot{H}_c is set to zero. That is to say, flight states are discontinuous at the end of the pullout maneuver, leading to an abrupt transition of the lift coefficient. Thus, the control action needs to offset the effect of the discontinuous flight states.

In this paper, the route parameters selected include that $H_d = 3200\text{m}$, $H_0 = 3030\text{m}$, $\dot{H}_0 = -50\text{m/s}$, $H_p = 2410\text{m}$, $H_m = 2300\text{m}$, so the trajectory with regard to the time change is shown in Figure 3.

From Figure 3, we find that the descent rate of the oriented route maintains -50m/s before 3.4s. Once the altitude reaches 3030m, the pullout maneuver starts, then the descent rate decreases continuously until it reaches the threshold (-7.53m/s) in 31s. At this time, the descent rate changes from -7.53m/s to 0 because the step transition occurs. Therefore, the control goal is that the real flight trajectory can track the planned route depicted in Figure 3, simultaneously the robust stability and quick dynamic response will be met for the pullout maneuver of Mars airplane.

4. Modeling and the Switching Control Law Design for Mars Airplane. Flight states of Mars airplane consist of the flight speed V , flight path angle γ , altitude h , angle of attack α and pitch angle rate q . Similarly, the longitudinal model is expressed by [24]

$$\begin{cases} \dot{V} = \frac{T \cos \alpha - D}{m} - g \sin \gamma \\ \dot{\gamma} = \frac{L + T \sin \alpha}{mV} - \frac{g \cos \gamma}{V} \\ \dot{q} = M_y / I_y \\ \dot{\alpha} = q - \dot{\gamma} \\ \dot{h} = V \sin \gamma \end{cases} \quad (6)$$

where the lift L , drag D , thrust T , pitching moment M_y is respectively calculated by

$$\begin{cases} L = \frac{1}{2}\rho v^2 S_w C_L \\ D = \frac{1}{2}\rho v^2 S_w C_D \\ M_y = \frac{1}{2}\rho v^2 S_w \bar{c} C_M \\ T = \delta_T \cdot T_{\max} \end{cases} \quad (7)$$

Once the lift coefficient C_L , drag coefficient C_D and pitching moment coefficient C_M are determined by the interpolation operation, the nonlinear model of Mars airplane is completely established. Moreover, the control inputs selected consist of the propulsive coefficient δ_T and actuator deflection angle δ_e in this paper, so the trim restriction conditions are concluded by

$$\begin{cases} \frac{T(\delta_{Tr}) \cos \alpha - D(V_r, h_r, \delta_{er}, \alpha_r)}{m} - g \sin \gamma_r = C_V \\ \frac{L(V_r, h_r, \delta_{er}, \alpha_r) + T(\delta_{Tr}) \sin \alpha_r}{m V_r} - \frac{g \cos \gamma_r}{V_r} = C_\gamma \\ M_y(V_r, h_r, \delta_{er}, \alpha_r) = 0 \end{cases} \quad (8)$$

where the subscript r represents the equilibrium flight state, then differentiating $\dot{h} = V \sin \gamma$, we have:

$$\begin{cases} C_V \sin \gamma_r + V_r \cos \gamma_r C_\gamma = 0 & H_c > H_0 \\ C_V \sin \gamma_r + V_r \cos \gamma_r C_\gamma = \frac{\dot{H}_0^2 (h_r - H_m)}{(H_0 - H_m)^2} & (H_c \leq H_0) \& \left(\left| \dot{H}_c \right| > \dot{H}_\varepsilon \right) \\ C_V = C_\gamma = \gamma_r = 0 & \left| \dot{H}_c \right| \leq \dot{H}_\varepsilon \end{cases} \quad (9)$$

According to Equations (8) and (9), four independent variables C_V , C_γ , δ_{er} , α_r can be solved completely for the oriented slide and pullout maneuver of Mars airplane. That is, the dynamic trim states are determined. Especially, the descent rate constantly

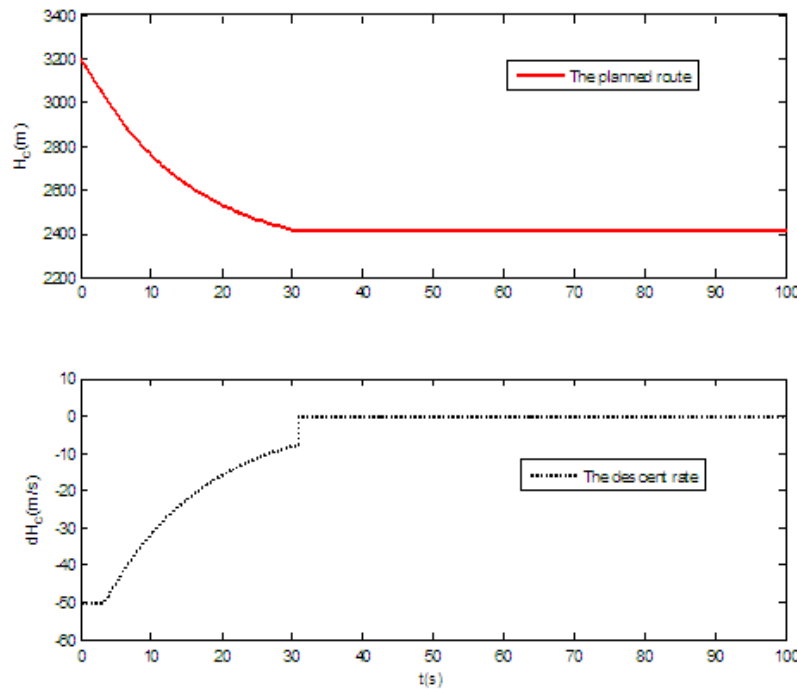


FIGURE 3. Planned route and descent rate with regard to the time change

decreases during the pullout maneuver, so the command of flight path angle gradually reduces concerning the small speed change. Furthermore, the total forces and moments are zeros at the horizontal flight stage because the thrust exists, then the equilibrium values δ_{er} , α_r , δ_{Tr} are obtained in line with the trim restriction condition.

Based on the flight characteristics and task requirements of the pullout maneuver, the control problems are generalized as follows:

1) It is in the low density atmospheric environment that the airplane executes a pullout maneuver, thus the low drag and high flight Mach enables that the acceleration into the unfavorable flight boundary is very easy if the pull-up process lasts too long. As a result, the anticipated control action should be fast and powerful to guarantee the stable performance throughout the flight range.

2) The change of flight states keeps continuous during the pullout maneuver in that the flight path angle of Mars airplane constantly decreases. Thus, the control action must be smooth and successive to track the given command signal.

3) The actuator control action is critical to adjust the speed change during the pullout maneuver because there is no thrust. By coordinating the relationship between the weight and drag, the goal that the flight speed first increases and then decreases is accomplished to guarantee the small change of the velocity during the pullout maneuver.

4) The control surfaces are used to orient Mars airplane itself before starting the pullout maneuver, then to implement the flight states switching at the end of the pullout maneuver. Therefore, the realization of the smooth transition depends on the feasible control system by adjusting the trim values, control parameters and even control structures with the change of the flight states.

Based on the above issues, the flight control laws are designed by steps. First aiming to the glide and pullout phase, the design idea of the control law reflects that the descent rate \dot{h} can follow the command signal for the implementation of the automatic pullout and the satisfaction of the quick responses. As a result, using the feedback of α and γ , the control law of the dynamic trim fight is proposed by

$$\begin{cases} \delta_{el} = \delta_{etrim} + k_{\alpha l}(\alpha - \alpha_{trim} - \alpha_{dl}) + k_{ql}q \\ \alpha_{dl} = K_{hil} \int (h - H_c) + K_{hl}(h - H_c) + K_{\gamma}(\gamma - \gamma_d) \end{cases} \quad (10)$$

where γ_d represents the command signal of the flight path angle, satisfying

$$\begin{cases} \gamma_d = \dot{H}_c/V \\ \alpha_{trim} = f_{\alpha}(V, h, \dot{h}) \\ \delta_{etrim} = f_{\delta e}(V, h, \dot{h}) \end{cases} \quad (11)$$

where α_{trim} and δ_{etrim} denote the trim angle of attack and actuator deflection with regard to any flight point, respectively. The control law design of the level flight is different from that of the pullout maneuver because the control goal is to maintain the static stability by the control action. For this reason, the control law of the level flight is presented by

$$\begin{cases} \delta_{ep} = \delta_{etrim} + k_{\theta p}(\theta - \theta_{trim} - \theta_{dp}) + k_{qp}q \\ \alpha_{dp} = K_{hip} \int (h - h_g) + K_{hp}(h - h_g) + K_{hdp}(\dot{h} - \dot{h}_d) \end{cases} \quad (12)$$

By comparing Equation (12) with Equation (10), we know that the different control modes including the different control structures and parameters are applied, thus the smooth transition is needed to avoid the unexpected response. Furthermore, in order to investigate the stability problems of the switched models for Mars airplane, the stability criteria in reference [25] is introduced in this paper. First, assumed that the flight velocity

is constant approximately for the pullout maneuver, we set

$$\begin{cases} V_p = (V_c \sin \gamma)^2 \\ 0 \leq \gamma_{\min} < \gamma < \gamma_{\max} < \pi/2 \end{cases} \quad (13)$$

Accordingly, there exist κ_1 and κ_2 such that it follows

$$\begin{cases} \kappa_1 \leq V_p < \kappa_2 \\ \kappa_1 = V_c^2 \gamma_{\min}^2 \\ \kappa_2 = V_c^2 \gamma_{\max}^2 \end{cases} \quad (14)$$

In addition, consider $\ddot{h} = V_c \cos \gamma \dot{\gamma}$, the differentiation of Equation (13) becomes

$$\dot{V}_p = V_c^2 \sin \gamma \cos \gamma \dot{\gamma} = V_c \sin \gamma \ddot{h} \quad (15)$$

Suppose that the flight altitude follows the command signal well due to the control action, then combined with Equation (3), we have

$$\begin{aligned} \dot{V}_p &= V_c \sin \gamma \ddot{h} = V_c \sin \gamma \ddot{H}_c = V_c \sin \gamma \frac{\dot{H}_0 \dot{H}_c}{(H_0 - H_m)} \\ &= V_c \sin \gamma \frac{\dot{H}_0 \dot{h}}{(H_0 - H_m)} = V_c^2 \sin^2 \gamma \frac{\dot{H}_0}{(H_0 - H_m)} = V_p^2 \frac{\dot{H}_0}{(H_0 - H_m)} \end{aligned} \quad (16)$$

Selecting $\lambda_p \geq \frac{\dot{H}_0}{H_m - H_0}$, we obtain

$$\dot{V}_p = V_p^2 \frac{\dot{H}_0}{(H_0 - H_m)} \leq -\lambda_p V_p^2 \quad (17)$$

Therefore, based on the Lemma 3 in reference [25], the system is globally uniformly exponentially stable for the switching signal with mode-dependent average dwell time

$$\tau_{ap} \geq \tau_{ap}^* = \frac{\ln \mu_p}{\lambda_p} \quad (18)$$

In this work, we adopt the switched link as follows

$$\begin{cases} \delta_e = D \delta_{el} + (1 - D) \delta_{ep} \\ D = \frac{a}{s+a} \text{sat} \left(\left| \dot{H}_c \right| > \dot{H}_\varepsilon \right) \end{cases} \quad (19)$$

where a represents the constant with regard to average dwell time τ_{ap} , and sat denotes the mode switching function. Correspondingly, the structure diagram of the switching control system can be given as follows.

5. Simulation. In this paper, the initial values of the simulation include that $Ma = 0.61$, $H_0 = 3200\text{m}$. Additionally, the original position of pullout maneuver is 3030m and the level flight height is 2410m . Also, Mars airplane properties are applied in Table 1 [9].

TABLE 1. Airplane properties

Property	Value	Units
Mass m	100	kg
Reference area S_w	7	m ²
Wing span b	6.25	m
Mean aerodynamic chord \bar{c}	1.25	m
Moment of inertia I_y	190	kg·m ²

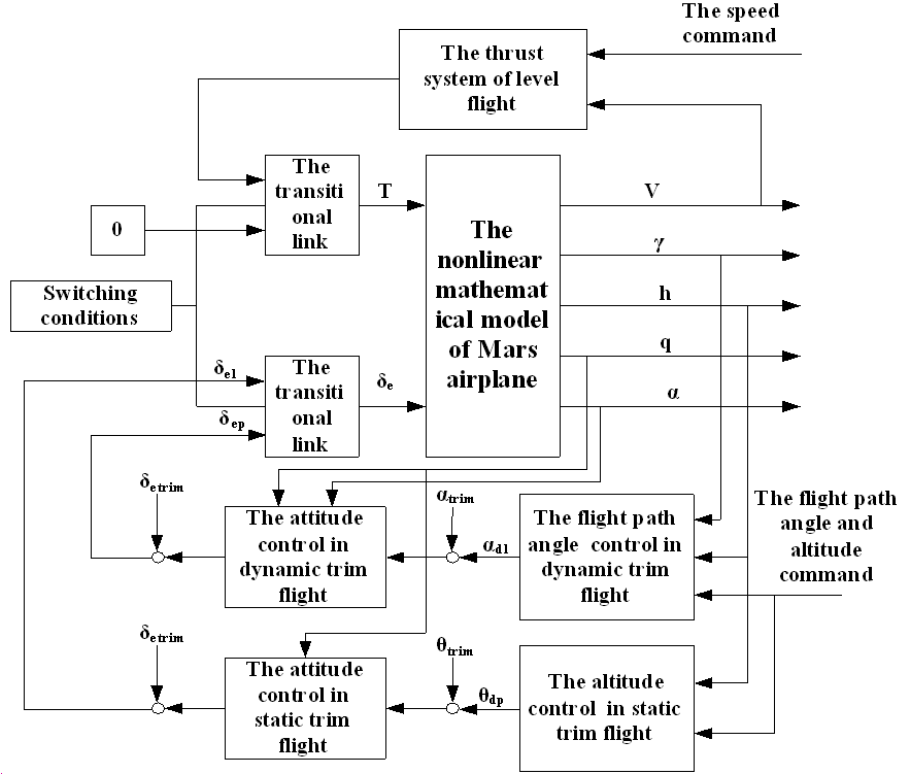


FIGURE 4. Structure diagram of switching control system for Mars airplane

From Table 1, some properties of Mars airplane are given to aid in the dimensionalizing of the aerodynamic forces and moments. To verify the feasibility of the proposed methods, the specific expressions of the altitude and its change rate command are given by

$$\dot{H}_c = \begin{cases} -50 & H_c > 3030 \\ \frac{-50(H_c - 2300)}{730} & (H_c \leq 3030) \& (|\dot{H}_c| > 7.53) \\ 0 & |\dot{H}_c| \leq 7.53 \end{cases} \quad (20)$$

$$H_c = \begin{cases} 3200 - 50t & H_c > 3030 \\ 2300 + 730e^{\frac{-50}{730}(t-3.4)} & (H_c \leq 3030) \& (|\dot{H}_c| > 7.53) \\ 2410 & |\dot{H}_c| \leq 7.53 \end{cases} \quad (21)$$

Then considering Equations (8) and (9), the dynamic and static trim states with regard to 0.62 Mach are calculated in Table 2.

From Table 2, we find that two abrupt transitions at altitude of 3030m and 2410m represent two switching processes among the slide, pullout and level flight. During the pullout maneuver, \dot{h} continually decreases, and V has the tendency of the increase first and reduction afterwards on behalf of the coordinated change relation between the drag and weight. Based on Table 2, the trim values with regard to the altitude are plotted in Figure 5.

According to Figure 5, two-step transitions appear at 3030m and 2410m due to the special flight tasks, also the trim states and control inputs vary when the flight altitude changes from 3200m to 2410m. Therefore, based on the trim state values, designing the feasible control system is necessary to provide reference flight states and maintain the flight stability.

TABLE 2. Dynamic and static trim states with regard to 0.62 Mach

h	\dot{h}	\ddot{h}	\dot{V}	γ	α	δ_e
(m)	(m/s)	(m/s ²)	(m/s ²)	(deg)	(deg)	(deg)
3200	-50.0	0	0.8725	-19.53	2.309	-1.547
3100	-50.0	0	0.8705	-19.53	2.270	-1.564
3030	-50.0	0	0.8690	-19.52	2.243	-1.575
3030	-50.0	3.425	0.6402	-19.52	6.699	0.043
2900	-41.1	2.815	0.4923	-15.93	5.663	-0.085
2800	-34.2	2.346	0.3511	-13.22	4.834	-0.389
2700	-27.4	1.877	0.2128	-10.53	4.071	-0.638
2600	-20.5	1.407	0.0673	-7.877	3.468	-0.934
2500	-13.7	0.938	-0.0807	-5.240	2.927	-1.240
2410	-7.53	0.516	-0.2131	-2.878	2.444	-1.487
2410	0	0	0	0	1.902	-1.699

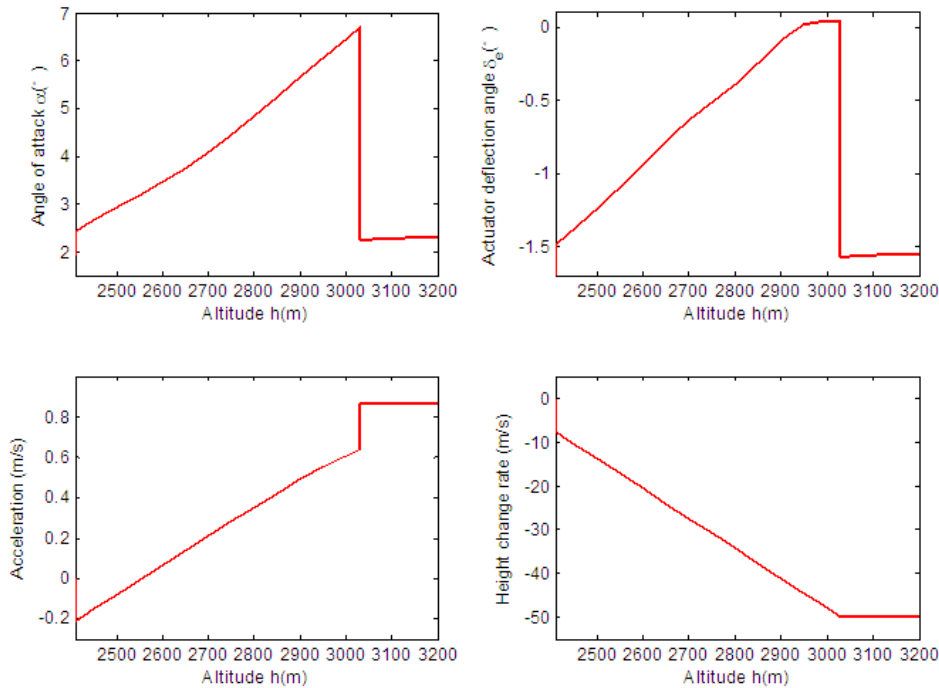


FIGURE 5. Trim states with regard to the altitude

In this paper, the control parameters in the simulation are selected in Table 3.

Based on Table 3, the control parameters are gotten by the trial-and-error methods that are simply understood and concisely checked. Furthermore, the airplane model and control system are built in MATLAB, then we assume that first Mars airplane flies with the glide slope to the height reaches 3030m, then pullout maneuver starts at the descent rate of -50m/s and terminates at altitude of 2410m, after that the level flight mode enables to hold the height. Accordingly, the simulation results are shown in Figure 6 and 7.

Figures 6 and 7 show the flight altitude and descent rate can track command signals well. Moreover, the unstable jumps are not induced by the state transitions with regard to the sliding, pullout and level flight. More importantly, the angle of attack and actuator

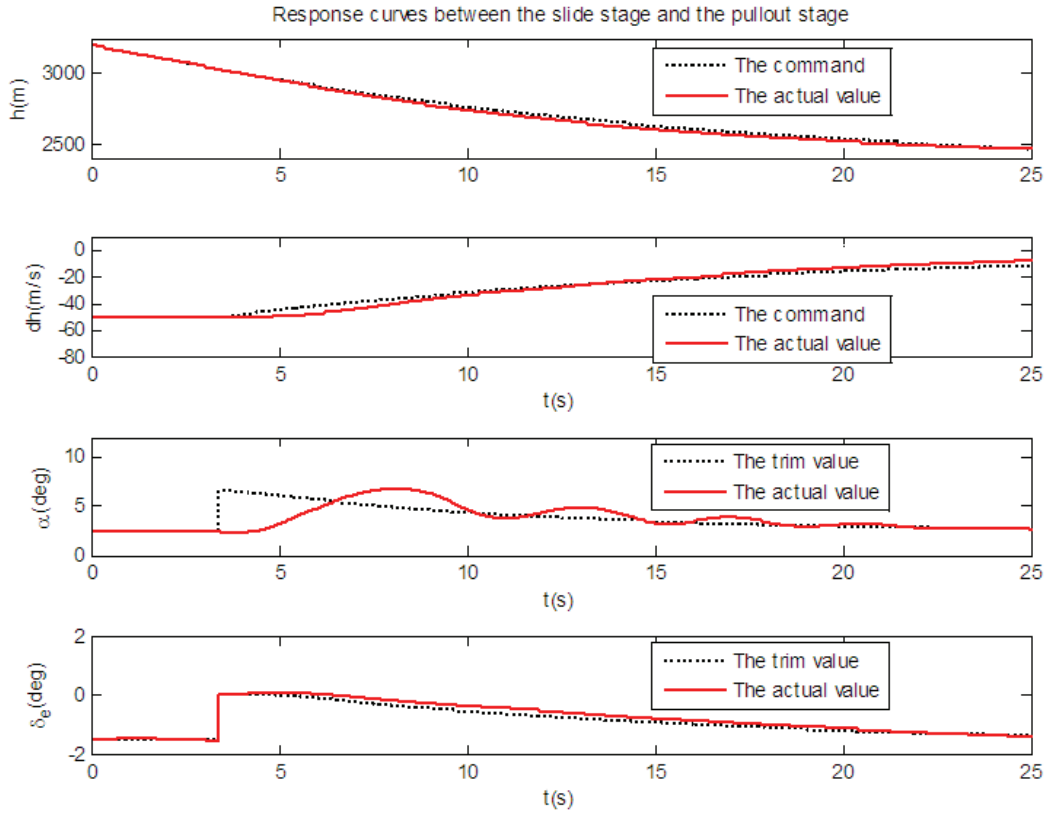


FIGURE 6. Response curves between the slide stage and pullout stage

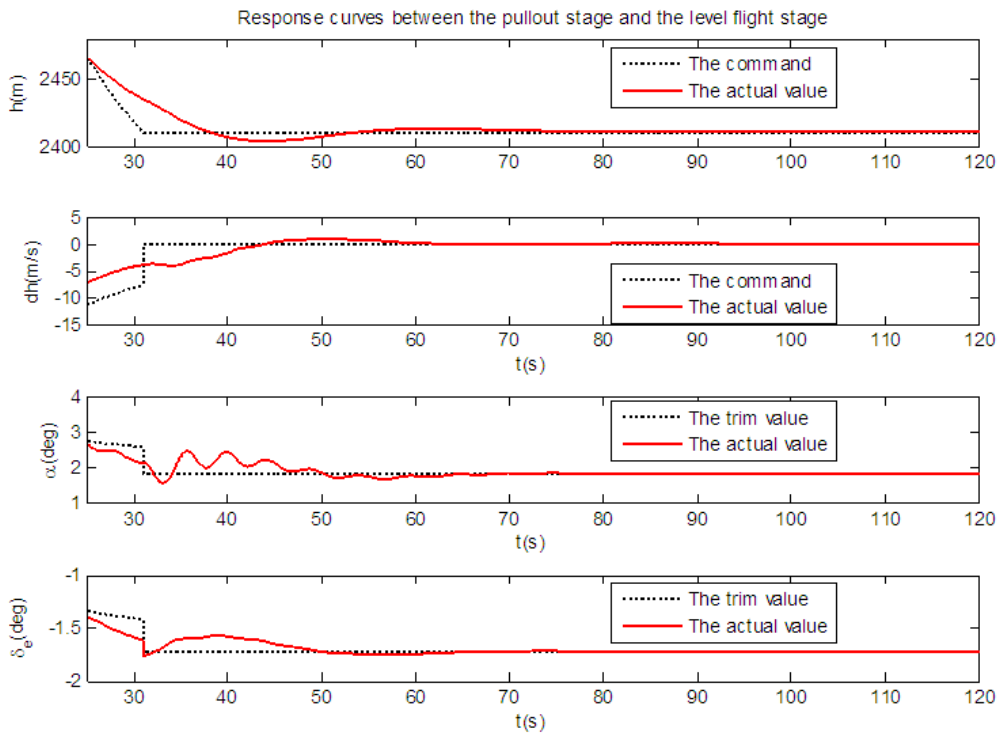


FIGURE 7. Response curves between the pullout stage and the level flight stage

TABLE 3. Control parameters selected in the simulation

Parameters	Values	Parameters	Values
$k_{\alpha l}$	0.002	$k_{\theta p}$	0.002
$k_{q l}$	0.001	$k_{q p}$	0.01
$K_{h i l}$	0.001	$K_{h i p}$	0.002
$K_{h l}$	0.05	$K_{h p}$	0.1
K_{γ}	0.3	$K_{h d p}$	0.5

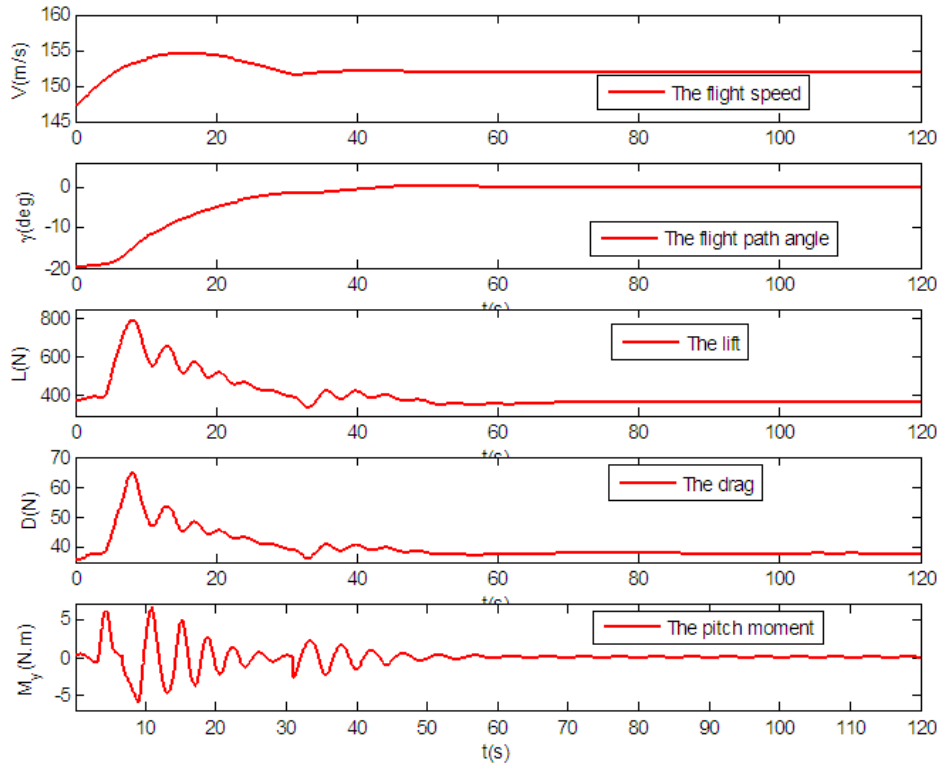


FIGURE 8. Response curves between the pullout stage and the level flight stage

deflection angle vary smoothly near trim values when motion modes is switching. And this demonstrates that the control action can ensure the stability and satisfy the accurate track demands throughout the whole flight range.

Furthermore, simulation results with regard to the speed, flight path angle, lift, drag and moment are obtained in Figure 8.

According to Figure 8, we find that the changes of the force and moment show the motion features at different flight stages. Especially, the speed and flight path angle continuously vary at the gliding and pull-up flight stage, whereas they are fixed values at the level flight stage. In addition, the force and moment converge towards constant values due to the control effects. This indicates that the motion can hold stable state ultimately and meet scientific investigation needs for the level flight by applying the switching control laws.

6. Conclusion. In this paper, the main works are to study and design the decoupling control system based on the switch control methods. First, the comparison of the flight

environment is carried out between on Mars and on Earth. Then, the mission of Mars airplane is described, and the flight trajectory is planned. Afterwards, the aerodynamics characteristic has been analyzed based on the established vehicle model. After that, the flight control laws are presented to guarantee the implementation of the smooth switching process. Finally, simulations validate the feasibility of the switching control methods. We believe the decoupling control methods proposed in this paper can provide the new design ideas for the other airplanes to meet the complicated task requirements in future.

Acknowledgment. This work is supported by China National Overseas Fund under Grant 201203070130, Doctoral Program Foundation of Institutions of Higher Education of China under Grant 20093218120035, NUAAs research funding under Grant NS2012044. The authors thank the editors and the reviewers for their help and improvements to the quality of our presentation.

REFERENCES

- [1] D. B. Robert, S. W. Henry, A. C. Mark et al., Design of the ARES Mars airplane and mission architecture, *Journal of Spacecraft and Rockets*, vol.43, no.5, pp.1026-1034, 2006.
- [2] N. Brown, A. Samuel and C. Richard, Mars exploration airplane: Design, construction, and flight testing of a stability, control, and performance demonstrator, *Proc. of AIAA Infotech Aerospace 2007 Conference and Exhibit*, Rohnert Park, CA, USA, 2007.
- [3] S. C. Smith, A. S. Hahn, W. R. Johnson et al., The design of the canyon flyer, *Proc. of the 38th AIAA Aerospace Sciences Meeting*, Reno, NV, USA, 2000.
- [4] J. C. Ledé, R. Parks and M. A. Croom, High altitude drop testing in Mars relevant conditions for the ARES Mars scout mission, *Proc. of the 2nd AIAA "Unmanned Unlimited" Systems, Technologies, and Operations – Aerospace, Land, and Sea Conference*, San Diego, CA, USA, 2003.
- [5] M. D. Guynn, M. A. Croom, S. C. Smith et al., Evolution of a MARS airplane concept for the AERS MARS scout mission, *Proc. of the 2nd AIAA "Unmanned Unlimited" Systems, Technologies, and Operations – Aerospace, Land, and Sea Conference*, San Diego, CA, USA, 2003.
- [6] P. S. Kenney and M. A. Croom, Simulation the ARES aircraft in the Mars environment, *Proc. of the 2nd AIAA "Unmanned Unlimited" Systems, Technologies, and Operations – Aerospace, Land, and Sea Conference*, San Diego, CA, USA, 2003.
- [7] H. N. Entry, Descent and deployment multi-body simulation for the ARES Mars airplane, *Proc. of the AIAA Infotech Aerospace Conference*, Seattle, Washington, USA, 2009.
- [8] J. E. Murray and V. Paul, Development of a Mars airplane entry, descent, and flight trajectory, *Proc. of the 39th Aerospace Sciences Meeting and Exhibit*, Reno, NV, USA, 2001.
- [9] M. Ganet, S. Joner and E. Ferrerira, Control design for a Mars Ascent Vehicle, *Proceedings of AIAA Guidance, Navigation, and Control Conference and Exhibit*, Keystone, CO, USA, 2006.
- [10] A. Hjartarson, Y. Paw and A. Chakraborty, Modeling and control design for the ARES aircraft, model-based aerospace challenge #1, *Proc. of AIAA Guidance, Navigation and Control Conference and Exhibit*, Honolulu, HI, USA, 2008.
- [11] R. Bhattacharya, J. Valasek, B. Singh et al., On modeling and robust control of ARES, *Proc. of AIAA Guidance, Navigation and Control Conference and Exhibit*, Honolulu, HI, USA, 2008.
- [12] D. Wang, P. Shi, W. Wang and J. Wang, Delay-dependent exponential H-infinity filtering for discrete-time switched delay systems, *Int. J. of Robust and Nonlinear Control*, vol.22, no.13, pp.1522-1536, 2012.
- [13] J. P. Henpanha and A. S. Morse, Stability of switched systems with average dwell time, *Proc. of the 38th IEEE Conference Decision and Control*, Phoenix, AZ, USA, 1999.
- [14] X. Zhao, L. Zhang, P. Shi and M. Liu, Stability of switched positive linear systems with average dwell time switching, *Automatica*, vol.48, no.6, pp.1132-1137, 2012.
- [15] B. Wang, P. Shi and J. Wang, Novel LMI-based stability and stabilization analysis on impulsive switched system with time delays, *J. of Franklin Institute*, vol.349, pp.2650-2663, 2012.
- [16] Z. Wu, P. Shi, H. Su and J. Chu, Delay-dependent stability analysis for switched neural networks with time-varying delay, *IEEE Trans. on Systems, Man and Cybernetics, Part B: Cybernetics*, vol.41, no.6, pp.1522-1530, 2011.
- [17] L. Zhang and P. Shi, L2-L-infinity model reduction for switched LPV systems with average dwell time, *IEEE Trans. on Automatic Control*, vol.53, no.10, pp.2443-2448, 2008.

- [18] L. Zhang and P. Shi, Stability, l_2 -gain and asynchronous H-infinity control of discrete-time switched systems with average dwell time, *IEEE Trans. on Automatic Control*, vol.54, no.9, pp.2193-2200, 2009.
- [19] D. Wang, P. Shi and W. Wang, Robust fault detection for continue-time switched delay systems: An linear matrix approach, *IET Control Theory and Applications*, vol.4, no.1, pp.100-108, 2010.
- [20] M. Mahmoud and P. Shi, Asynchronous H-infinity filtering of discrete-time switched systems, *Signal Processing*, vol.92, no.10, pp.2356-2364, 2012.
- [21] R. R. Reuben and R. O. John, Modeling approach for analysis and optimization of a long-duration Mars airplane, *Proc. of the 10th AIAA/ISSMO Multidisciplinary Analysis and Optimization Conference*, Albany, NY, USA, 2004.
- [22] S. C. Smith, M. D. Guynn and C. L. Streett, MARS airplane airfoil design with application to ARES, *Proc. of the 2nd AIAA "Unmanned Unlimited" Systems, Technologies, and Operations – Aerospace, Land, and Sea Conference, Workshop and Exhibition*, San Diego, CA, USA, 2003.
- [23] C. A. Kuhl, Design of a Mars airplane propulsion system for the aerial regional-scale environmental survey (ARES) mission concept, *Proc. of the 44th AIAA/ASME/SAE/ASEE Joint Propulsion Conference & Exhibit*, Hartford, CT, USA, 2008.
- [24] L. Fiorentini, A. Serrani, M. A. Bolender and D. B. Doman, Nonlinear robust adaptive control of flexible air-breathing hypersonic vehicles, *Journal of Guidance, Control, and Dynamics*, vol.32, no.2, pp.401-416, 2009.
- [25] X. Zhao, L. Zhang, P. Shi and M. Liu, Stability and stabilization of switched linear systems with mode-dependent average dwell time, *IEEE Trans. on Automatic Control*, vol.57, no.7, pp.1809-1815, 2012.